Published in final edited form as:
Neuropharmacology. 2007 February ; 52(2): 562–575.

Functional selectivity of dopamine D_1 receptor agonists in regulating the fate of internalized receptors *

Jessica P. Ryman-Rasmussen[1], **Adam Griffith**[2], **Scott Oloff**[1], **Nagarajan Vaidehi**[2], **Justin T. Brown**[1], **William A. Goddard III**[2], and **Richard B. Mailman**[1]

1 *University of North Carolina at Chapel Hill, Curriculum in Toxicology (JPR-R), Departments of Pharmacology (SO, JB, RBM) and Psychiatry, Neurology and Medicinal Chemistry (RBM), Chapel Hill, NC 27599*

2 *Materials and Process Simulation Center, California Institute of Technology, Pasadena, California 91125*

Abstract

Recently, we demonstrated that D_1 agonists can cause functionally selective effects when the endpoints of receptor internalization and adenylate cyclase activation are compared. The present study was designed to probe the phenomenon of functional selectivity at the D_1 receptor further by testing the hypothesis that structurally dissimilar agonists with efficacies at these endpoints that equal or exceed those of dopamine would differ in ability to influence receptor fate after internalization, a functional endpoint largely unexplored for the D_1 receptor. We selected two novel agonists of therapeutic interest that meet these criteria (the isochroman A-77636, and the isoquinoline dinapsoline), and compared the fates of the D_1 receptor after internalization in response to these two compounds with that of dopamine. We found that dopamine caused the receptor to be rapidly recycled to the cell surface within 1 h of removal. Conversely, A-77636 caused the receptor to be retained intracellularly up to 48 h after agonist removal. Most surprisingly, the D_1 receptor recovered to the cell surface 48 h after removal of dinapsoline. Taken together, these data indicate that these agonists target the D_1 receptor to different intracellular trafficking pathways, demonstrating that the phenomenon of functional selectivity at the D_1 receptor is operative for cellular events that are temporally downstream of immediate receptor activation. We hypothesize that these differential effects result from interactions of the synthetic ligands with aspects of the D_1 receptor that are distal from the ligand binding domain.

Introduction

The dopamine receptors are a superfamily of heptahelical G protein-coupled receptors (GPCRs) that have historically been partitioned into "D_1-like" and "D_2-like" subfamilies (Kebabian and Calne, 1979; Garau *et al.*, 1978). The dopamine D_1 receptor is a member of the "D_1-like" subfamily, and couples to adenylate cyclase through stimulatory G proteins G_s and

Address all correspondence to: Dr. Richard B. Mailman, CB #7160, University of North Carolina School of Medicine, Chapel Hill, NC 27599-7160, VOICE: 919-966-2484; FAX: 919-966-9604; EMAIL: Richard_Mailman@med.unc.edu.

Reprint requests should be sent to Dr. Richard B. Mailman; CB#7160, University of North Carolina, School of Medicine; Chapel Hill, NC 27599-7160, Richard_mailman@med.unc.edu.

Richard B. Mailman and the University of North Carolina at Chapel Hill have a financial interest in Biovalve Technologies, Inc. that holds license rights to dinapsoline. All opinions are those of the authors, and do not represent those of that company, the University of North Carolina at Chapel Hill, or the California Institute of Technology.

G_{olf} (Herve *et al.*, 1993). The early steps in the regulation of the D_1 receptor following the binding of dopamine have been addressed in model cell lines. After the binding of dopamine to the D_1 receptor, receptor phosphorylation is complete within minutes (Gardner et al. 2001). This can be mediated by GRKs (Gardner *et al.*, 2001; Tiberi *et al.*, 1996) and/or protein kinase A (PKA) (Mason *et al.*, 2002). Both types of kinases may facilitate D_1 desensitization, and the contribution of each to the overall extent of receptor phosphorylation and desensitization is probably highly dependant on the cell line being studied. Receptor phosphorylation allows arrestin to bind to the third intracellular loop of the receptor (Kim *et al.*, 2004) leading to D_1 receptor internalization. Arrestin is not trafficked into the cell with the receptor, thus the D_1 receptor is considered a "Class A" GPCR (Oakley *et al.*, 2000). Following dopamine-induced internalization, the D_1 receptor is rapidly recycled back to the cell surface (Vickery and von Zastrow, 1999; Vargas and von Zastrow, 2004). Recent studies indicate that a signal sequence within the proximal C-terminal region of the receptor mediates this process (Vargas and von Zastrow, 2004).

The effects of D_1 agonists other than dopamine itself on regulatory events downstream of receptor activation are not well characterized. Besides heuristic interest in these questions, several of the D_1 agonists that have been tested as antiparkinson agents in human and non-human primates caused a very rapid tolerance evidenced as an almost complete loss of response within a day or so (Asin and Wirtshafter, 1993; Kebabian *et al.*, 1992; Lin *et al.*, 1996; DeNinno *et al.*, 1991a; Johnson *et al.*, 1992). Thus, such molecular events may be important in understanding the cellular mechanisms that contribute to the development of this therapeutic tolerance. Previously, we have observed that desensitization of adenylate cyclase responsivity and receptor down-regulation are highly dependent upon the agonist used, but largely independent of adenylate cyclase activity and agonist affinity in a stably transfected C6 glioma cell line (Lewis *et al.*, 1998). Recently, we explored the relationship between agonist structure, receptor affinity, and efficacy of receptor internalization and adenylate cyclase activation in greater depth by constructing an HEK cell line stably transfected with a hemaglutinin-tagged human D_1 receptor and comparing these endpoints in 13 agonists from three different structural families. We found that D_1 agonists exhibit functional selectivity at these early endpoints following receptor activation that are apparently independent of agonist structure or binding affinity (Ryman-Rasmussen *et al.*, 2005).

These results suggested the major hypothesis tested herein, that D_1 agonists are functionally selective in regulating receptor function at the endpoint of intracellular trafficking of the D_1 receptor, an endpoint that temporally lies downstream of adenylate cyclase activation and internalization, events more immediate of receptor activation. We selected two agonists of therapeutic interest, A-77636 and dinapsoline (DNS), for comparison with dopamine at this endpoint. Both of these synthetic ligands have efficacies of internalization and adenylate cyclase activation comparable to that of dopamine in the HA-hD_1 HEK cell line (Ryman-Rasmussen *et al.*, 2005). The isochroman A-77636 elicits profound and rapid *in vivo* tolerance occurring within approximately 24 h, preventing its use in Parkinson's disease therapy (Lin *et al.*, 1996). Conversely, DNS does not cause such tolerance in a rat model of Parkinson's disease (Gulwadi *et al.*, 2001). The mechanisms of tolerance are unknown, but presumably result from cellular adaptations that lie temporally downstream of receptor internalization and adenylate cyclase activation.. The current data demonstrate that although these agonists cause functional changes identical to dopamine immediately following receptor binding, with time they modify D_1 receptor trafficking, and thus show a novel pattern of functional selectivity.

Methods

Materials

Dopamine and A-77636 [(−)-(1R,3S)-3-adamantyl-1-(aminomethyl)-3,4-dihydro-5,6-dihydroxy-1H-2-benzopyran hydrochloride)] were purchased from RBI/Sigma-Aldrich (St. Louis, MO). Dinapsoline (8,9-dihydroxy-2,3,7, 11b-tetrahydro-1H-naph[1,2,3-de] isoquinoline) and [^{3}H] SCH23390 were synthesized according to published procedures (Ghosh *et al*., 1996; Wyrick *et al*., 1986). All other reagents and materials were from Sigma Chemical Company (St. Louis, MO), unless otherwise stated.

HA-hD$_1$ HEK model cell line

The HA-hD$_1$ HEK cell line was constructed as described previously (Ryman-Rasmussen *et al.*, 2005). Cells were maintained in DMEM-H, 10% FBS, 100 U/mL penicillin, 100 μg/mL streptomycin, and 0.6 mg/mL geneticin at 37ºC and 5% CO_2. Assay plates were coated with 4 μg/mL human fibronectin (Enzyme Research Laboratories Inc., South Bend, IN) at 37º C for 1 h or overnight, followed by addition of polylysine to 0.2 mg/mL for an additional 30 min to prevent cell loss. Coating medium was aspirated and cells were immediately plated at a density of 500–1000 cells per mm^2.

Radioreceptor assays

HA-hD$_1$ receptor expression level and affinity for dopamine, A-77636, and DNS were determined by saturation binding and competition assays. Membrane homogenates from HA-hD$_1$ HEK cells were prepared as previously described (Lewis *et al.*, 1998). Receptor density and affinity of SCH23390 were measured by incubation of membrane homogenates in 0 to 2 nM [^{3}H]SCH23390 in 50 mM HEPES, 4 mM $MgCl_2$, 0.01% ascorbic acid, pH 7.4 for 15 min at 37ºC. Yohimbine and propranolol (50 nM) were included to block endogenous adrenergic receptors. Non-specific binding was determined by parallel incubations with 1 μM SCH23390. Radioreceptor assays were done using either a Molecular Dynamics/Skatron harvester and LKB 1209 RackBeta counter, or a Packard 96 Filtermate Harvester and TopCount Counter, using appropriate glass fiber filters and scintillation fluid. The total protein concentration of membrane preparations used in the saturation binding assays was determined by use of the BCA^{TM} assay according to manufacturer's instructions (Pierce, Rockford, IL). Affinity of dopamine, A-77636, and DNS for the HA-hD$_1$ receptor was determined by competition (10^{-10} to 10^{-4} M) versus 0.3 nM [^{3}H]SCH23390 in the presence of 50 nM propranolol and yohimbine.

Adenylate cyclase functional potency and efficacy

Adenylate cyclase activation by dopamine, A-77636, and DNS was measured in whole HA-hD$_1$ HEK cells as previously described (Ryman-Rasmussen *et al.*, 2005). Triplicate wells in 24 well plates were untreated or incubated with increasing concentrations of dopamine, A-77636, or DNS in the presence of 500 μM IBMX at 37ºC for 15 min. Duplicate wells at the highest concentration of agonist included the D$_1$ receptor-selective antagonist, 50 μM SCH23390, as a negative control. All wells contained 50 nM (S)-propranolol and yohimbine to antagonize endogenous β-adrenergic receptors. The reaction was quenched with 0.1 N HCl, and cAMP was quantified by a modified radioimmunoassay based on a previously published method (Harper and Brooker, 1975).

Internalization assays

Internalization time-course assays were performed as previously described (Ryman-Rasmussen *et al.*, 2005). Briefly, 24-well plates of 1 d post-confluent HA-hD$_1$ HEK cells were adapted to treatment medium (L15 medium, 20 mM HEPES, 0.01% ascorbic acid pH 7.4) for

1 h. One plate per treatment time point was used. Each plate contained control wells for no drug (N=6), drug plus antagonist (N=2), and drug alone (N=4 per drug). Dopamine, A77636, or DNS were added to cells a final concentration of 10 μM. For wells containing drug plus antagonist, the final antagonist concentration (SCH23390 or butaclamol) was 50 μM. (S)-propranolol and yohimbine were included in all wells at a final concentration of 50 nM to block endogenous adrenergic receptors. Plates were incubated for 0 to 120 min in a 37ºC water bath, rapidly cooled on ice, and fixed in 4% paraformaldehyde buffered with 0.1N sodium phosphate prior to analysis for cell surface receptors by RIA vs. the HA-epitope. Internalization dose-response assays were performed by treating HA-hD_1 HEK cells with increasing concentrations (10^{-10} to 10^{-3} M) of dopamine, A-77636, or DNS at 37ºC for 1 h in the presence of 50 nM -(S)-propranolol and yohimbine in (N=4). All assays also contained control wells for no agonist (N=6) and 10 μM agonist plus 50 μM of the antagonist, SCH23390 (N=2 per drug). At the end of the incubation period, cells were fixed, and processed for a cell surface RIA of HA-hD_1 using a primary antibody for the HA epitope as previously described (Ryman-Rasmussen *et al.*, 2005). All data were expressed as a percentage of untreated controls.

Assays for cell surface receptor recovery

Twenty-four well plates of 1 d post-confluent HA-hD_1 HEK cells were adapted to treatment medium (DMEM-H medium, 20 mM HEPES, 0.01% ascorbic acid pH 7.4) for 1 h. One plate per treatment time point was used. Each plate contained control wells for No drug (N=6), and drug and antagonist (N=2 per drug) in addition to drug treatment wells (N=4 per drug). Dopamine, A-77636, or DNS were added to a final concentration of 10 μM. For wells containing drug and antagonist, the final antagonist concentration (SCH23390 or butaclamol) was 50 μM. (S)(−)propranolol and yohimbine were included in all wells at a final concentration of 50 nM to block endogenous adrenergic receptors. Plates were incubated for 1 h at 37ºC and 5% CO_2. Drug treatment medium was then aspirated, and cells were rinsed once with sterile PBS prior to incubation in treatment medium without drug from 0 to 48 h. Cells were then rapidly cooled on ice, and fixed in 4% paraformaldehyde buffered with 0.1N sodium phosphate prior to analysis for cell surface receptors by RIA for the HA epitope as previously described (Ryman-Rasmussen *et al.*, 2005). Protein synthesis inhibition studies with 5 μM actinomycin D (Calbiochem) were performed similarly, with the antibiotic added to the medium after agonist removal.

Biotinylation studies

A modification of a previously published procedure was followed (Pan *et al.*, 2003). EZ-Link Sulfo-NHS-SS-Biotin™ (Pierce, Rockford IL) was freshly dissolved at 4–5 mg/mL in 20 mM sodium phosphate buffer with 120 mM NaCl, pH 8.0 (at 4ºC). Twelve well plates of 1 d post-confluent HA-hD_1 HEK cells were washed twice with cold PBS, and biotinylated with 0.5 mL of reagent for 60 min on ice. The reaction was quenched by addition of 1% BSA and 10 mM glycine in sodium phosphate/NaCl for 10 min. The biotinylated cells were rinsed twice with cold PBS, and adapted for 1 h at 37ºC in L15 medium with 20 mM HEPES, 0.01% ascorbic acid, pH 7.4. Dopamine was added to the drug treatment wells to a final concentration of 10 μM, with propranolol and yohimbine present at 50 nM each. Plates were incubated for 1 h at 37ºC. Cells then were washed twice in cold PBS, and biotinylated cell surface receptors were cleaved by two rounds of incubation in fresh 150 mM reduced glutathione (GSH)/150 mM NaCl pH 8.8–8.9 (at 0ºC) on ice for 15 min. Cells were rinsed twice with cold PBS, and drug free medium added, after which they either were placed on ice (0 hr) or incubated an additional 1 h at 37ºC. At the end of the incubation, cells were returned to ice. Cells were washed twice in cold PBS, and another two rounds of incubation in fresh 150 mM GSH/150 mM NaCl pH 8.8–8.9 (at 0ºC) were performed in wells assaying for recycled, biotinylated receptor. Cells were lysed in 1 mL 10 mM HEPES, 2 mM EDTA, 0.5% Triton X-100, 0.1% SDS pH 7.4 with 0.5 mM PMSF, passed through a 26G needle, and incubated an additional 1h at 4ºC to solubilize

receptors. Samples were centrifuged at 14,000g for 15 min. A 20 μl aliquot of the supernatant was saved for determination of protein concentration, and 900 μl of the supernatant was transferred to new 1.5 mL tubes containing 75 μL of ImmunoPure Immobilized Avidin (Pierce Biochemical, Rockford IL). Binding to the avidin resin proceeded for 2 h on a rotating platform at 4ºC. Avidin resin was washed twice with lysis buffer and resuspended in 70 μL of Laemlli buffer. Based on protein content prior to resin binding, approximately 35 μl of each sample was separated on a 4–12% denaturing polyacrylamide gel (Novex/Invitrogen), and blotted onto a PVDF membrane. Samples were blotted to a primary HA.11 antibody (Covance, Inc, from mouse raw ascites) at a 1000-fold dilution followed by detection with a secondary rabbit anti-mouse antibody conjugated to horseradish peroxidase (BioRad). Bands were revealed by chemiluminescent detection (ECL^{TM}System, Amersham) and exposure to film (BioFilm, Denville Scientific).

Determination of protein synthesis inhibition with [^{35}S]-methionine

Twenty-four well plates were washed twice with sterile PBS. Then [^{35}S]-methionine (1000 μCi/ml Amersham) was added to DMEM-H medium buffered with 20 mM HEPES and 0.01% ascorbic acid pH 7.4, with and without 5 μM actinomycin D to a final concentration of 2 nM, and incubated 24 or 48 h. Replicate wells for cell viability assays without [^{35}S]-methionine were also included in the experiment. At the end of the incubation period, cells were washed twice with PBS. [^{35}S]-methionine-labeled cells were lysed in 10 mM HEPES, 2 mM EDTA, 0.5% Triton X-100, 0.1% SDS, pH 7.4, and an aliquot counted on a beta counter (RackBeta). Similarly-treated, non-radioactive cells were washed twice with PBS. MTT (thiazolyl blue) was added to DMEM at 250μg/mL, and applied to cells for 15 min. Cells were rinsed twice with PBS. DMSO was added to the wells to solubilize the precipitate and plates were placed on a rocker platform for 15 min. Aliquots from the wells were read in a spectrophotometer (BioRad) at 595 nm (Twentyman and Luscombe, 1987). The amount of [^{35}S]-methionine in actinomycin D-treated and untreated wells was normalized to the absorbance of MTT in similarly treated wells. Data were expressed as a percentage of samples untreated with actinomycin D.

Metabolic labeling of HA-hD$_1$ with [^{35}S]-methionine

Six-well plates of 85% confluent HA-hD$_1$ HEK cells were starved for 6–8 h in methionine-free DMEM medium (Specialty Media/Cell and Molecular Technologies, Inc.) containing 100 U/mL penicillin, 100 μg/mL streptomycin, and 0.6 mg/mL geneticin. “Starving medium” containing 10% FBS, 10 μM cold methionine, and 0.02–0.04μM [^{35}S]-methionine (Amersham-Pharmacia) were added to the cells for 18 h. After labeling, cells were washed three times with sterile PBS, and equilibrated in DMEM-H medium, 20 mM HEPES, 0.01% ascorbic acid, pH 7.4, containing 0.6 mM cold methionine. Drug treatment and recovery studies were done as described earlier, except methionine levels in the medium were maintained at 0.6 mM (normally 0.2 mM). At the end of the recovery studies, cells were rinsed twice with cold PBS, lysed in RIPA buffer with 0.5 mM PMSF containing 100 U/mL DNAse and 1 mg/mL RNAse (Boehringer Mannheim), and scraped into 1.5 mL tubes. Tubes were incubated at 4ºC on a rotary platform for 1 h to solubilize receptors and digest nucleic acids. Tubes were centrifuged at 14,000 g, and 800 μl was transferred to new 1.5 mL tubes. A 20 μL aliquot was saved for determination of protein content. ^{35}[S]-Met-HA-hD$_1$ was immunoprecipitated by a procedure similar to one published previously (Tiberi *et al.*, 1996). Twenty μl of Protein G-Sepharose (Amersham Pharmacia) was added to each tube, and the tubes were incubated at 4ºC on a rotary platform for 1 h to pre-clear the supernatant. The supernatant again was transferred to a new tube, a 100-fold dilution of the HA.11 primary antibody was added to each tube, and samples were incubated for 2 h at 4ºC on a rotary platform. Fifty μL of Protein G-Sepharose was added to each tube, and incubation continued for 1 h. Immunoprecipitated samples were washed three times with RIPA, and the immunoprecipitate resuspended in 25

μL Laemlli buffer. The same amount of total protein (ca. 25 μL) was loaded on 4–12% denaturing polyacrylamide gel (Novex/Invitrogen), and the gel run according to the manufacturer's instructions. The gel was fixed for 1 h in a 20% methanol, 10% acetic acid solution, and dried on a gel drier (BioRad). Dried gels were exposed to PhosphorImager plates (Molecular Dynamics/Amersham Biosciences, Piscataway, NJ) and exposed for 2–4 days. Images were scanned on a Typhoon Imager (Molecular Dynamics), and band densities quantified with ImageQuant™ (Amersham Biosciences) software based on average number of pixels per band.

Confocal microscopy

HA-hD_1 HEK cells were grown to 50% confluency on glass coverslips coated with fibronectin and polylysine in 24-well plates. Cells were treated in duplicate with either dopamine, A77636, or DNS (all at 10 μM) for 1 h in the presence of 50 nM (S)-propranolol and yohimbine, as described above. Cells were rinsed with PBS, and returned to the incubator for assessment of cell surface recovery at 1 h, 12 h and 48 h, as described above. At the end of the recovery assay, cells were fixed in ice-cold, freshly made methanol-free 4% paraformaldehyde buffered in 0.1 N sodium phosphate (pH 7.4) on the bench for 30 min. Fixed cells were rinsed twice with PBS, and permeabilized with 0.3% Triton X-100 in DMEM/50 mM HEPES/10% FBS for 30 min on ice to allow antibody access to receptors on the cellular interior. Permeabilized cells were blocked with 5% BSA in DMEM/50 mM HEPES/10% FBS for 30 min, and incubated with a 1:1,000 dilution of the HA.11 primary antibody (from mouse raw ascites, Covance, Inc.) as described above. Detection was by 1 h incubation with a secondary rat anti-mouse antibody conjugated to the Cy3 fluorophore (Jackson Immunolabs). Coverslips were rinsed with PBS, and wet-mounted with DAPI-containing Vectashield™ medium (Vector Labs, Inc.). Slides were scanned in 0.6 μm steps on an upright Leica SP2 confocal microscope with a 63 X (oil) Plan Apo objective (NA 1.4 to 0.6). The DAPI fluorophore was excited with a 351/364 nm UV laser line and the cy3 fluorophore with a 568 nm krypton laser line. Detection was in tunable channels optimized for the emission of these fluorophores, with no observable fluorophore overlap. Images represent the cellular interior, approximately midway through the thickness of the cells. Data are representative of three independent experiments conducted at different times.

Molecular modeling

We predicted the three-dimensional structure of human dopamine D_1 receptor using the MembStruk method (Trabanino *et al.*, 2004). We then used the HierDock ligand docking method (Vaidehi *et al.*, 2002) to locate the binding region for dopamine, for the two stereoisomers of dinapsoline and for four diastereomers of A-77636. We then predicted the details of the binding site for these ligands (allowing protein side chains to change and the backbone to relax), and calculated their binding energies (details of the structure and binding site to be published elsewhere).

Displacement radioreceptor assay

HEK 293 cells stably expressing the hD_1-wild-type receptor were harvested to produce membranes for use in receptor binding assays. 100 mM culture dishes containing the HEK cells were washed with ice cold PBS 1X and then lysed for ~15 min. with 3 mL ice cold lysis buffer (10mM Hepes, pH 7.4). Cells were scraped, transferred to centrifuge tubes and spun at 28,000 g for 20 min. Pellets were then transferred to a Wheaton Glass/Teflon homogenizer in 10 mM Hepes buffer, and homogenized five times. Homogenization and centrifugation was repeated for a total of two times. The final pellet was resuspended in storage buffer (20 mM Hepes, 250 mM sucrose, pH 7.4), aliquoted in 1 mL microcentrifuge tubes and snap-frozen. Membrane aliquots were stored at −80 C until use.

For use, membranes were thawed, washed, resuspended in assay buffer (50 mM HEPES/4 mM $MgCl_2$, pH 7.4), and then divided into four aliquots of 500 μL each. The following was added to each aliquot at a final concentration of 10 μM: I) A77636; II) dinapsoline; III) dopamine; and IV) Buffer only. All samples were incubated at 37°C for 15 min. Upon termination of the incubation, each sample was washed twice by centrifugation at 5000 g for 5 min and resuspended in buffer. Each aliquot was then resuspended in 5 mL of buffer containing phenylmethanesulfonyl fluoride, and incubated for 60 min at 37°C. The samples were washed once more by centrifugation and resuspended in assay buffer. Samples (250 μL) were then tested for binding capacity (500 μL final assay volume) using 0.5 nM and 5 nM [^{3}H]SCH23390 (i.e., 1*K_D and 5*K_D) to label D_1 receptors. Half of the tubes also contained 1 μM unlabeled SCH23390 to estimate non-specific binding. Binding was initiated by the addition of tissue to the tubes, and after incubation for 15 min at 37°C, the reaction was terminated by filtering with ice-cold buffer on a Packard Filtermate cell harvester (Packard Instruments, Downers Grove, IL). Radioactivity was measured using a Packard TopCount Microplate Scintillation and Luminescence Counter.

Data and statistical analysis

Affinity data were fit first to a sigmoidal model of variable slope. The data then were resolved assuming a two-site model, to yield a $K_{D(high)}$ and $K_{D(low)}$ and percent of sites in each state. $K_{0.5}$ values were calculated from the IC50s using the bimolecular competitive model from Cheng and Prusoff (1973). The data for adenylate cyclase potency were expressed as the percentage of cAMP produced at the highest concentration of agonist used and the data for internalization potency expressed as percentage cell surface receptors of untreated controls. The data for both of these functional endpoints were fit to a sigmoidal dose-response curve. All of the analyses of these dose-response data were performed using Prism Ver. 3 or 4 (GraphPad, Inc, San Diego CA). An ANOVA with a post-hoc Tukey test was used to compare means for all internalization and recovery experiments. Significance was set at $p<0.05$. All statistical testing was done using Systat Version 6 software (Systat Software Inc., Point Richmond CA).

Results

Radioreceptor assays

Saturation binding with the D_1-selective antagonist, [3H] SCH23390, in membrane homogenates indicated that the assay expression level of HA-hD_1 in this cell line is approximately 4 ± 1 pmol/mg membrane protein with a K_D of 2.4 ± 0.8 nM (Figure 1, Panel A and Table 1). Competition assays of dopamine, A-77636, and DNS versus [^{3}H] SCH23390 were performed to determine the affinities of these compounds for the HA-hD_1 receptor (Figure 1, Panel B and Table 1). Dopamine and DNS best fit a two-site binding model, whereas A-77636 best fit a one-site model. These values are in agreement with results previously obtained in this model cell line (Ryman-Rasmussen *et al.*, 2005) and those published results in rat striatal homogenates and in vitro expression systems (Ghosh *et al.*, 1996;Lewis *et al.*, 1998).

Internalization time course of HA-hD_1

We characterized the temporal course of receptor internalization in response to these three agonists. Internalization for all three agonists is best described as a first-order process with a half-life of less than 10 min that reaches a steady-state by 30 min that is stable to at least 2 h (Figure 2A).

A one-hour agonist treatment time was chosen for subsequent studies because it is midway through the observed steady state (see Figure 2A). At this time, steady state levels of cell surface

HA-hD_1 differ significantly between agonists (Figure 2B). An average of 78 ± 6% of cell surface HA-hD_1 remain after treatment with dopamine, compared to 69 ± 3% after treatment with DNS, and 62 ± 3% after treatment with A-77636 (see legend of Figure 2 for statistics). The loss of cell surface HA-hD_1 in response to all three agonists was blocked with the D_1 selective antagonist, SCH 23390, consistent with the hypothesis that this process is mediated through activation of the D_1 receptor.

Adenylate cyclase and internalization functional potency and efficacy

Adenylate cyclase functional potency and efficacy were then assessed for all three agonists in whole cells (Figure 3, Panel A). Dopamine had an EC50 of 91 ± 47 nM versus 5.7 ± 1.8 nM for A-77636 and 10 ± 3.0 nM for DNS. A-77636 and DNS also had full intrinsic activity relative to dopamine, in agreement with previous work (DeNinno *et al.*, 1991b;Lewis *et al.*, 1998;Ghosh *et al.*, 1996;Ryman-Rasmussen *et al.*, 2005). Additionally, D_1-mediated activation of adenylate cyclase for all three agonists was completely blocked by the D_1-selective antagonist SCH23390 (data not shown).

The rank order of efficacy in eliciting an internalization response was A-77636 > DNS > dopamine (Figure 2, Panel B). The functional potencies of internalization also were determined for each agonist (Figure 3, Panel B). Dopamine had an EC50 of 600 ± 200 nM versus 80 ± 10 nM for A-77636 and 200 ± 100 nM for DNS.

Rapid recycling of HA-hD_1 to the cell surface after treatment with dopamine

HA-hD_1 HEK cells were treated with 10 μM dopamine, A-77636, or DNS for 1 h, rinsed with PBS, and incubated in drug-free medium for 0 to 48 h. As shown in Figure 4, 1 h after removal of dopamine, HA-hD_1 was significantly recovered to the cell surface ($p<0.001$) to levels that are undistinguishable from control values. Conversely, no recovery of cell surface HA-hD_1 was observed at this time point after removal of either A-77636 or DNS. In fact, a significant decrease in cell surface HA-hD_1 was observed for both agonists (A-77636: $p<0.001$; DNS: $p<0.05$).

We hypothesized that recovery of the HA-hD_1 receptor in response to dopamine was the result of receptor recycling, based on previous reports (Vickery and von Zastrow, 1999; Vargas and von Zastrow, 2004). We therefore used a cell impermeable, cleavable biotinylation reagent to label all cell surface receptors prior to agonist treatment. This assay allows cleavage of non-internalized receptors by glutathione (GSH) after agonist treatment, so that only the fate of internalized receptors is tracked. Internalized receptors were isolated rapidly by binding to avidin-Sepharose, and the HA-hD_1 receptor identified by Western blotting with an HA.11 antibody. Thus, the fate of internalized HA-hD_1 was tracked unequivocally, and other mechanisms (e.g., new receptor biosynthesis or export of cytosolic receptors to the surface) ruled out (Figure 5). Efficient labeling of cell surface HA-hD_1 was achieved (Lane 2) with low background (Lane 1), and the signal in the absence of dopamine (Lane 2) was mostly eliminated by cleavage with GSH (Lane 3). One h after treatment with 10 μM DA and cleavage of cell surface HA-hD_1 with GSH, there was internalization of HA-hD_1 (Lane 4). One h after removal of DA from the drug treatment medium, a band corresponding to HA-hD_1 was present on the surface and interior of the cell (Lane 6). After cleavage with GSH, the remaining receptors on the interior of the cell (Lane 7) were significantly reduced relative to the total present (Lane 6), but were slightly increased compared to control levels (Lane 5). Thus, the difference in band density between Lanes 6 and 7 can be mainly attributed to recycled HA-hD_1. These data indicate that the majority of HA-hD_1 was recycled back to the cell surface within 1 h of removal of DA from the culture medium. Unfortunately, this method could not be applied to assess the fate of internalized HA-hD_1 in response to A77636 and DNS, possibly as a result of hydrolysis

of the disulfide bond in the cleavable biotin label in cellular compartments or from prolonged (up to 48 h) incubation times (data not shown).

Delayed responses of HA-hD$_1$ following removal of A-77636 or DNS

The differences observed 1 h after agonist removal from the culture medium raised questions about drug-specific differences over time. Thus, cell surface HA-hD$_1$ receptors were examined at later time points after removal of these agonists. Significant decreases in cell surface HA-hD$_1$ were observed at 24, 36, and 48 h after removal of A-77636, whereas for DNS, there was a small but significant increase in cell surface HA-hD$_1$ by 48 h (Figure 6, Panel A). Comparison of the 0 and 48 h time points (Figure 6, Panel B) shows that 48 h after removal of A-77636, cell surface HA-hD$_1$ decreased from 65 ± 2% to 46 ± 3% ($p<0.001$). Conversely, there was a significant increase in cell surface HA-hD$_1$ after removal of DNS, from 73 ± 2% to 82 ± 5% ($p<0.05$). Thus, after DNS-treatment, cell surface receptors were still significantly decreased relative to untreated controls at 48 h ($p<0.001$), but were significantly greater than in cells treated with A-77636 ($p<0.001$).

Delayed recovery of HA-hD$_1$ is independent of new protein synthesis

This most logical explanation for an increase in cell surface HA-hD$_1$ density 48 h after removal of DNS from the medium is new receptor biosynthesis. Cell surface biotinylation studies could have ruled this out unequivocally, but could not be used due to hydrolysis of the label during the extended length of the experiment. Therefore, we utilized protein synthesis inhibition to determine if protein synthesis was required for receptor recovery 48 h after DNS treatment. Cycloheximide was first tried, but was too cytotoxic in this cell line at efficacious concentrations (data not shown). We therefore used Actinomycin D. The maximum tolerated concentration of actinomycin D in this cell line for 48 h was 5 μM (data not shown). Inhibition of protein synthesis was determined quantitatively by metabolic labeling studies with [^{35}S]-methionine. Actinomycin D treatment caused noticeable differences in the confluency of these cells after 48 h of treatment, compared to untreated controls (data not shown), and so determination of the degree of inhibition of protein synthesis required normalization to the number of viable cells. An MTT cell viability assay was used for this purpose. Based on comparison of incorporated [^{35}S]-methionine in actinomycin D-treated and untreated controls, new protein synthesis was inhibited 31 ± 1.2% within 24 h and 45 ± 2.2% within 48 h by actinomycin D (Figure 7 Panel A). Replacement of the cell culture medium at 24 h with a fresh actinomycin D did not significantly decrease the incorporation of [^{35}S]-methionine at 48 h (data not shown). As shown in Figure 7, Panel B, inclusion of actinomycin D in the medium after agonist removal causes no significant change in the cell surface HA-hD$_1$ response resulting from treatment with dopamine, A-77636, or DNS, indicating that new protein synthesis did not mediate receptor recovery to the cell surface after removal of DNS from the culture medium.

Metabolically labeled D$_1$ receptors after 48 h

Although protein synthesis inhibition by Actinomycin D was significant, it was not complete, and could not completely rule out new receptor biosynthesis as the mechanism by which cell surface HA-hD$_1$ density is recovered. It also could not rule out an alternative mechanism of export of cytosolic receptors to the cell surface. We therefore pursued pulse-chase experiments in which cellular proteins were “pulsed” with [^{35}S]-methionine and “chased” with an excess of cold methionine prior to HA-hD$_1$ receptor internalization and recovery assays in response to agonists. At the end of the recovery period, radiolabeled receptors were recovered by immunoprecipitation. Thus, the same pool of cell surface HA-hD$_1$ present at the time of agonist exposure could be followed over 48 h. These experiments showed that the [^{35}S]-met HA-

hD_1 present during agonist exposure was present 48 h after agonist removal. A similar result was obtained for untreated controls (Figure 8, Panels A and B).

Visualization of receptor localization by confocal microscopy

The previous, quantitative assays provided valuable evidence of rapid HA-hD_1 recovery to the cell surface in response to dopamine, delayed recovery in response to DNS, and no recovery in response to A77636. These quantitative data gave no indication of whether or not these agonists might cause differential localization of the receptor within the cell. We therefore visualized HA-hD_1 receptor localization in permeabilized cells by confocal microscopy at various time points after agonist removal from the culture medium (Figure 9). In the absence of agonist, the HA-hD_1 receptor was localized primarily to the cell membrane. After 1 h treatment with 10 μM dopamine, the HA-hD_1 receptor localizes to a large endosomal-like structure outside the nucleus. This occurred with a concomitant decrease in cell surface receptor staining. One h after dopamine was removed, HA-hD_1 cell surface receptor density recovered to levels similar to that observed in untreated controls and the large endosomal-like structure was absent. Treatment of HA-hD_1 HEK with 10 μM A-77636 or DNS clearly show that surface receptors recover much slowly with DNS or not at all with A-77636. One h after A-77636 treatment, a pronounced loss in cell surface staining for HA-hD_1 receptors was apparent and internalized receptors were localized to numerous, large endosomal-like structures on the interior of the cell. Cell surface HA-hD_1 receptor density did not recover within the 48 h observation period. One h after DNS treatment, the HA-hD_1 receptor staining was evident in numerous, fused endosomal-like structures. A large endosomal-like structure was well-defined at 12 h and persisted at 24 h, at which time some cell surface HA-hD_1 staining was observed (data not shown). At 48 h, recovery of cell surface HA-hD_1 staining was apparent and the large endosomal-like structure was absent.

Molecular modeling of the D_1 receptor

The *in vitro* data strongly suggested that agonist structure might be the determinate that affected the differential trafficking of the D_1 receptor. To explore the molecular factors that make A-77636 and dinapsoline traffic the D_1 receptor so differently from each other and from dopamine, we examined the differences in the D_1 binding site of dopamine, dinapsoline and A-77636. For all three ligands [S(+) dinapsoline, (1R,3S) A-77636, and dopamine] the predicted binding site in the D_1 receptor involves several common elements. These include amino acids in TM3 [V100(3.29), D103(3.32), and I104(3.33)], in TM5 [S199(5.43), S202 (5.46), F203(5.47)], in TM6 [F288(6.51), L291(6.54), N292(6.55)], and in TM7; [F313(7.35), V317(7.39)]. This model shows several predicted differences in the binding site for A-77636 and for dopamine. These arise from N97(3.26) on TM3; F156(4.58), V159(4.61) and W163 (4.65) on TM4; A195(5.39), V200(5.44) on TM5; L291(6.54) and L295(6.58) on TM6; and F313(7.35) and V317(7.39) on TM7. These residues all have favorable van der Waals interaction with A-77636 (~6 Kcal/mol more so than for dopamine). Predicted contributions to differential binding of dinapsoline and dopamine arise from I104(3.33) on TM3, F156(4.58) on TM4, V200(5.44) and F203(5.47) on TM5, and P287 on TM6, providing ~3 Kcal/mol better interaction energy to the D_1 receptor. Figure 10 shows that the adamantyl group of A-77636 protrudes from the extracellular domain of D_1 receptor to interact with W163(4.65) on TM4. Thus the accessory hydrophobic adamantyl group of A77636 may be stabilized by the extracellular loops in a way that markedly decreases ligand dissociation.

Displacement results consistent with limited dissociation of A-77636 from the D_1 receptor

It has been hypothesized that A-77636 dissociates slowly from the D_1 receptor, but this based solely on indirect evidence that there is continued accumulation of cAMP after apparent removal of drug (Lin *et al.*, 1996). To provide additional direct evidence for this hypothesis,

we used the strategy of radioligand displacement. Either A-77636 (1 μM) or buffer (as vehicle) was incubated with striatal membranes for 15 min, the membranes were diluted, allowed to equilibrate, washed, and then assayed for available D_1-like binding sites. As shown in Figure 12, membranes pretreated with A-77636 showed a dramatic reduction in the number of available SCH23390 binding sites even after repeated washing and dilution. For the untreated membranes, or those pretreated with DA or DNS, the data fit a one-site binding model with an R^2 >0.94 for each case. In addition, the K_D for [^{3}H]SCH23390 was essentially identical for control membranes (0.51 ± 0.09 nM) versus ones pretreated with DNS (0.41 ± 0.07 nM) or DA (0.29 ± 0.05 nM), but the estimated K_D for the A77636 treated membranes had a 95% confidence interval that included 0. These results are consistent with the hypothesis from the model outlined in the previous section.

Discussion

Utilizing an HA-hD_1 HEK cell line (Ryman-Rasmussen *et al.*, 2005), we studied the intracellular trafficking of the D_1 receptor following binding of dopamine and two structurally dissimilar agonists, A-77636 and DNS. These agonists were similarly efficacious to dopamine in activating adenylate cyclase, and caused a similar time course of D_1 receptor internalization. Conversely, the synthetic agonists had quite different effects on events that were not temporally proximal to initial receptor occupation. The current study investigated these interesting differences in D_1 receptor trafficking using a variety of endpoints that probed cell surface D_1 receptor density in response to agonist activation.

We first characterized the time-course of internalization of the HA-hD_1 receptor in response to dopamine, A-77636, or DNS. In all cases, internalization was best described as a first-order process that reached a steady-state by 30 min and was then constant until 2 h. Whereas DNS was of similar efficacy to dopamine in causing internalization in this cell line, A-77636 caused significantly greater internalization, essentially acting like a “super agonist” at this function, but not at adenylate cyclase. The rank order of potency (A-77636 ≥ DNS ≫dopamine) was similar at internalization and adenylate cyclase activation, although both A-77636 and DNS had somewhat lower potency at the former. From this data, we established for all three agonists that a 1 h treatment time at a concentration that gave high occupancy (10 μM) was sufficient to achieve steady-state levels of D_1 receptor internalization. This provided the basis for assessing post-endocytic agonist effects on receptor trafficking.

The cell surface RIA data, in conjunction with confocal microscopy, showed that HA-hD_1 receptor density was recovered on the cell surface 1 h after removal of dopamine, indicating that the D_1 receptor rapidly recycled in this cell line after binding dopamine. Alternative explanations, such as export of cytosolic receptors to the cell surface or, less likely, protein biosynthesis, were ruled out by the use of a cell impermeable, cleavable biotinylation reagent. This demonstrated unequivocally that recovery of the receptor to the cell surface in response to dopamine was a result of receptor recycling. These data were consistent with earlier studies that showed that D_1 receptor is recycled rapidly back to the surface of HEK cells after dopamine removal (Vickery and von Zastrow, 1999; Vargas and von Zastrow, 2004).

Conversely, treatment with A-77636 had a very different effect on HA-hD_1 receptor localization. After a 1 h treatment with A-77636 and removal of free drug, neither cell surface RIA, nor confocal microscopy, showed evidence of recovery to the cell surface in the next 48 h. The cell surface RIA data showed a significant decline in cell surface receptor number between 24 and 48 h after removal of A-77636. This sustained loss of cell surface receptors after the PBS wash and subsequent incubation in drug-free medium was probably due to continued receptor internalization as a result of the very slow dissociation of A-77636 from the receptor (Figure 12 and Lin *et al.*, 1996). Further support for our hypothesis on the persistent

receptor internalization came from pulse-chase studies with [^{35}S]-methionine that demonstrated that roughly half of the A-77636-treated HA-hD_1 was still present 48 h after agonist removal. Additionally, the confocal data demonstrated that A-77636 targets the receptor to numerous endosomal-like structures within the cell after 1 h of agonist treatment, structures that were still visible 48 h later. Taken together, these data indicate that the retained receptor (likely complexed with agonist) is resistant to degradation. This result is unexpected, since GPCRs that are not recycled are usually rapidly degraded. The persistence of the D_1 receptor intracellularly after treatment with A-77636 may be explained by the unusual resistance of the receptor to proteolysis (Vargas and von Zastrow, 2004). As an aside, our data showing inability of A-77636 to dissociate from the D_1 receptor in washed membranes rules out receptor phosphorylation or other enzyme catalyzed events in the most proximal mechanism involved in this unusual trafficking.

Another unexpected finding was observed with DNS. The cell surface RIA data indicates that DNS caused very delayed recovery of cell surface HA-hD_1 receptor density. This result was supported by the confocal data that showed that DNS caused localization of the receptor to a large endosomal-like structure after 1 h of treatment. Following removal of DNS from the culture medium, this endosomal-like structure was still evident at 12 and 24 h, indicating that the receptor was not degraded. Forty-eight h after DNS removal, this endosomal-like structure was absent and receptor staining was recovered on the cell surface.

Such a delay between receptor internalization and recovery of D_1 receptors after DNS treatment is, to our knowledge, highly unusual for a recycled GPCR. Therefore, we tested the alternative hypothesis that new protein biosynthesis was responsible for the delayed HA-hD_1 receptor recovery following DNS treatment. Use of actinomycin D resulted in 45% inhibition of protein synthesis without marked effects on cell viability. The 24–48 h interval during which protein synthesis inhibition occurred corresponded to the time during which recovery of HA-hD_1 receptor density to the cell surface was seen after DNS removal. The actinomycin D, however, had no effect on cell surface HA-hD_1 recovery. These data were consistent with the hypothesis that new protein biosynthesis was not the mechanism responsible for the cell surface recovery of the HA-hD_1 receptor following DNS removal. To provide additional evidence, we conducted pulse-chase studies with [^{35}S]-methionine to determine if the original pool of HA-hD_1 present prior to DNS treatment was still present 48 h later. These data demonstrated that roughly 50% of the original receptors were indeed present at this time point. Taken together, these data strongly indicated that the delay in recovery of the D_1 receptor to the cell surface after treatment with DNS resulted from receptor recycling. The metabolic labeling studies also indicated that roughly half of the original pool of HA-hD_1 receptor present prior to treatment with all agonists was still present 48 h later, a result that was observed in both untreated cells and cells treated for 1 h with dopamine, A-77636, or DNS. This result indicates that 1 h of exposure to these agonists is not sufficient to accelerate or decelerate the rate of receptor turnover in this cell line. Slow turnover of the receptor is expected under these experimental conditions because serum and selective antibiotic are absent from the medium during this time.

The apparent ability of dopamine, A-77636, and DNS to cause differential effects in the intracellular trafficking of the D_1 receptor despite their very similar acute functional effects raises two important questions: what structural features of the ligands are responsible for the unique actions of the synthetic agonists, and what domains of the receptor are involved in this transduction. One hypothesis that should be tested further is the relative role of ligand dissociation on these trafficking changes. Dopamine, the smallest and most hydrophilic of these agonists, is the one that causes most rapid receptor recycling, whereas A-77636 and DNS more hydrophobic, and also are hypothesized to engage additional aspects of the receptor. Our data (Figure 12), coupled with that of Lin et al. (1996), provide compelling evidence that A-77636 persists on the D_1 receptor for long periods of time and cannot be removed by thorough washing

of membranes or by competition with excesses of antagonist. Our docking studies of A77636 in the predicted structure of the D_1 receptor (see Figure 10) support the suggestions from previous experiments (Mottola *et al.*, 1996; Grubbs *et al.*, 2004; Ghosh *et al.*, 1996; Mailman *et al.*, 1998) that the accessory hydrophobic adamantyl group of A77636 is stabilized by residues near the extracellular domain sufficiently to eliminate dissociation. For example, we predict that the adamantyl group in A-77636 ligand interacts with V159, W163 on TM4 and L291, L295 on TM6, with these residues in the extracellular end of the TM regions contributing 6 Kcal/mol extra stabilization (i.e., enthalpic contributions but not entropic or temperature dependent terms) to binding of A-77636, but none for dopamine. In our ligand docking calculations, we scanned the entire receptor structure for locating the possible binding site(s) of the ligands A-77636, dinapsoline, and dopamine. For dinapsoline and A-77636, apart from the binding site between TMs 3, 4, 5 and 6 described above (shown in Figure 11, left), we found a much weaker but perhaps significant secondary binding site for dopamine was in the intracellular portion of the inter-helical regions of TM 3, 4, 5 and 6 (see Figure 11, right). Although we have not characterized this site computationally, the observation suggests that there could be an allosteric binding site that recognizes the endogenous agonist to play a role in reformation of the receptor. This site might not be recognized by other agonists (such as dinapsoline and A-77636], perhaps explaining the low degree of dissociation and its subsequent effects on receptor recovery.

If further research confirms that slow dissociation of D_1 ligands is a key initiating factor that results in dramatically altered patterns of receptor trafficking, then the underlying mechanisms would be of importance. Agonist dissociation may be necessary in order for the sorting sequence in the proximal C-terminus of the D_1 receptor to interact with the endosomal sorting machinery that targets the receptor to a rapid recycling pathway (Vargas and von Zastrow, 2004). In addition, dissociation of the agonist may be required to mediate arrestin dissociation from the receptor (or vice-versa). Arrestin is not trafficked into the cell with the D_1 receptor in response to dopamine (Zhang *et al.*, 1999). Thus, in the case of dopamine, the D_1 receptor fits the profile of a “Class A” GPCR. “Class B” GPCRs, in contrast, are still associated with arrestin when they are internalized and the cycling of this class of receptors is much slower (Oakley *et al.*, 2000). An inability of the agonist-receptor-arrestin complex to dissociate upon internalization, possibly as a result of stabilization of the arrestin-receptor complex by a ligand like A-77636 could thus be hypothesized to “convert” a Class A GPCR to a Class B GPCR. The persistence of HA-hD_1 intracellularly as a result of treatment with A-77636, or to a lesser extent, DNS provides some evidence that this could happen. It would be ideal to be able to measure the intracellular concentrations of ligand directly, but chemical methods are not adequately sensitive, and would be confounded by trapped (non-specific) ligand. Moreover, the current data show that post-treatment that includes washing and competition from antagonists cannot remove the ligand even at short time intervals, let alone after the receptor has been trafficked away from the cell surface.

In summary, this study shows that structurally dissimilar D_1 agonists that are similar in terms of their acute functional profile (e.g., adenylate cyclase) are functionally selective (Simmons, 2005; Mailman and Gay, 2004; Urban *et al.*, 2006) in regard to long-term receptor trafficking. These findings open the door to future mechanistic studies in three distinct areas. First, what are the important ligand-receptor interactions that allow ligand-specific differentiation of long-term trafficking for compounds that otherwise appear functionally similar. Second, what intracellular mechanisms are involved in the unusual trafficking of such novel ligand-receptor complexes. Finally, do the involved intracellular mechanisms provide a clue as to the reason that A-77636 causes profound motor tolerance *in vivo* over a similar time course to that studied here. Investigation into all three areas will help define the universality of this phenomenon and its overall physiological importance.

Acknowledgements

The confocal data were obtained at the Michael Hooker Microscopy Facility at UNC-Chapel Hill. This work was supported by NIH research grants NS039036 (RM), MH040537 (RM), and MH073910 (WCG,RM), and training grants ES007126 and NS007431.

References

Asin KE, Wirtshafter D. Effects of repeated dopamine D_1 receptor stimulation on rotation and c-fos expression. Eur J Pharmacol 1993;235:167–168. [PubMed: 8100194]

Cheng Y, Prusoff WH. Relationship between the inhibition constant (K_I) and the concentration of inhibitor which causes 50 per cent inhibition (I50) of an enzymatic reaction. Biochem Pharmacol 1973;22:3099–3108. [PubMed: 4202581]

DeNinno MP, Schoenleber R, MacKenzie R, Britton DR, Asin KE, Briggs C, Trugman JM, Ackerman M, Artman L, Bednarz L. A68930: a potent agonist selective for the dopamine D1 receptor. Eur J Pharmacol 1991a;199:209–219. [PubMed: 1683288]

DeNinno MP, Schoenleber R, Perner RJ, Lijewski L, Asin KE, Britton DR, MacKenzie R, Kebabian JW. Synthesis and dopaminergic activity of 3-substituted 1-(aminomethyl)-3,4-dihydro-5,6-dihydroxy-1H-2-benzopyrans: characterization of an auxiliary binding region in the D1 receptor. J Med Chem 1991b;34:2561–2569. [PubMed: 1652023]

Garau L, Govoni S, Stefanini E, Trabucchi M, Spano PF. Dopamine receptors: pharmacological and anatomical evidences indicate that two distinct dopamine receptor populations are present in rat striatum. Life Sci 1978;23:1745–1750. [PubMed: 723447]

Gardner B, Liu ZF, Jiang D, Sibley DR. The role of phosphorylation/dephosphorylation in agonist-induced desensitization of D1 dopamine receptor function: evidence for a novel pathway for receptor dephosphorylation. Mol Pharmacol 2001;59:310–321. [PubMed: 11160868]

Ghosh D, Snyder SE, Watts VJ, Mailman RB, Nichols DE. 9-Dihydroxy-2,3,7,11b-tetrahydro-1H-naph [1,2,3-de]isoquinoline: a potent full dopamine D1 agonist containing a rigid-beta-phenyldopamine pharmacophore. J Med Chem 1996;39:549–555. [PubMed: 8558526]

Grubbs RA, Lewis MM, Owens-Vance C, Gay EA, Jassen AK, Mailman RB, Nichols DE. 8,9-dihydroxy-1,2,3,11b-tetrahydrochromeno[4,3,2,-de]isoquinoline (dinoxyline), a high affinity and potent agonist at all dopamine receptor isoforms. Bioorg Med Chem 2004;12:1403–1412. [PubMed: 15018913]

Gulwadi AG, Korpinen CD, Mailman RB, Nichols DE, Sit SY, Taber MT. Dinapsoline: characterization of a D_1 dopamine receptor agonist in a rat model of Parkinson's disease. J Pharmacol Exp Ther 2001;296:338–344. [PubMed: 11160615]

Harper JF, Brooker G. Femtomole sensitive radioimmunoassay for cyclic AMP and cyclic GMP after 2′-O-acetylation by acetic anhydride in aqueous solution. J Cyc Nuc Res 1975;1:207–218.

Herve D, Levi-Strauss M, Marey-Semper I, Verney C, Tassin JP, Glowinski J, Girault JA. G_{olf} and G_s in rat basal ganglia: possible involvement of G_{olf} in the coupling of dopamine D_1 receptor with adenylyl cyclase. J Neurosci 1993;13:2237–2248. [PubMed: 8478697]

Johnson KB, Criswell HE, Jensen KF, Simson PE, Mueller RA, Breese GR. Comparison of the D1-dopamine agonists SKF-38393 and A-68930 in neonatal 6-hydroxydopamine-lesioned rats: behavioral effects and induction of c-fos-like immunoreactivity. J Pharmacol Exp Ther 1992;262:855–865. [PubMed: 1354257]

Kebabian JW, Britton DR, DeNinno MP, Perner R, Smith L, Jenner P, Schoenleber R, Williams M. A-77636: a potent and selective dopamine D1 receptor agonist with antiparkinsonian activity in marmosets. Eur J Pharmacol 1992;229:203–209. [PubMed: 1362704]

Kebabian JW, Calne DB. Multiple receptors for dopamine. Nature 1979;277:93–96. [PubMed: 215920]

Kim OJ, Gardner BR, Williams DB, Marinec PS, Cabrera DM, Peters JD, Mak CC, Kim KM, Sibley DR. The role of phosphorylation in D1 dopamine receptor desensitization: evidence for a novel mechanism of arrestin association. J Biol Chem 2004;279:7999–8010. [PubMed: 14660631]

Lewis MM, Watts VJ, Lawler CP, Nichols DE, Mailman RB. Homologous desensitization of the D1A dopamine receptor: efficacy in causing desensitization dissociates from both receptor occupancy and functional potency. J Pharmacol Exp Ther 1998;286:345–353. [PubMed: 9655879]

Lin CW, Bianchi BR, Miller TR, Stashko MA, Wang SS, Curzon P, Bednarz L, Asin KE, Britton DR. Persistent activation of the dopamine D_1 receptor contributes to prolonged receptor desensitization: studies with A-77636. J Pharmacol Exp Ther 1996;276:1022–1029. [PubMed: 8786531]

Mailman RB, Gay EA. Novel mechanisms of drug action: functional selectivity at D_2 dopamine receptors (a lesson for drug discovery). Med Chem Res 2004;13:115–126.

Mailman, RB.; Nichols, DE.; Lewis, MM.; Blake, BL.; Lawler, CP. Functional Effects of Novel Dopamine Ligands: Dihydrexidine and Parkinson's Disease as a First Step. In: Jenner, P.; Demirdemar, R., editors. Dopamine Receptor Subtypes: From Basic Science to Clinical Application. IOS Stockton Press; 1998. p. 64-83.

Mason JN, Kozell LB, Neve KA. Regulation of dopamine D-1 receptor trafficking by protein kinase A-dependent phosphorylation. Mol Pharmacol 2002;61:806–816. [PubMed: 11901220]

Mottola DM, Laiter S, Watts VJ, Tropsha A, Wyrick SD, Nichols DE, Mailman RB. Conformational analysis of D_1 dopamine receptor agonists: pharmacophore assessment and receptor mapping. J Med Chem 1996;39:285–296. [PubMed: 8568818]

Oakley RH, Laporte SA, Holt JA, Caron MG, Barak LS. Differential affinities of visual arrestin, beta arrestin1, and beta arrestin2 for G protein-coupled receptors delineate two major classes of receptors. J Biol Chem 2000;275:17201–17210. [PubMed: 10748214]

Pan L, Gurevich EV, Gurevich VV. The nature of the arrestin x receptor complex determines the ultimate fate of the internalized receptor. J Biol Chem 2003;278:11623–11632. [PubMed: 12525498]

Ryman-Rasmussen JP, Nichols DE, Mailman RB. Differential activation of adenylate cyclase and receptor internalization by novel dopamine D1 receptor agonists. Mol Pharmacol 2005;68:1039–1048. [PubMed: 15985612]

Simmons MA. Functional selectivity, ligand-directed trafficking, conformation-specific agonism: What's in a name? Mol Interv 2005;5:154–157. [PubMed: 15994454]

Tiberi M, Nash SR, Bertrand L, Lefkowitz RJ, Caron MG. Differential regulation of dopamine D1A receptor responsiveness by various G protein-coupled receptor kinases. J Biol Chem 1996;271:3771–3778. [PubMed: 8631993]

Trabanino RJ, Hall SE, Vaidehi N, Floriano WB, Kam V, Goddard WA III. First principles predictions of the structure and function of G-protein coupled receptors: validation for bovine rhodopsin. Biophys J 2004;86:1904–1921. [PubMed: 15041637]

Twentyman PR, Luscombe M. A study of some variables in a tetrazolium dye (MTT) based assay for cell growth and chemosensitivity. Br J Cancer 1987;56:279–285. [PubMed: 3663476]

Urban JD, Clarke WP, von Zastrow M, Nichols DE, Kobilka BK, Weinstein H, Javitch JA, Roth BL, Christopoulos A, Sexton P, Miller K, Spedding M, Mailman RB. Functional selectivity and classical concepts of quantitative pharmacology. J Pharmacol Exp Ther. 2006

Vaidehi N, Floriano WB, Trabanino R, Hall SE, Freddolino P, Choi EJ, Zamanakos G, Goddard WA III. Prediction of structure and function of G protein-coupled receptors. Proc Natl Acad Sci U S A 2002;99:12622–12627. [PubMed: 12351677]

Vargas GA, von Zastrow M. Identification of a novel endocytic 'recycling signal' in the D_1 dopamine receptor. J Biol Chem. 2004

Vickery RG, von Zastrow M. Distinct dynamin-dependent and -independent mechanisms target structurally homologous dopamine receptors to different endocytic membranes. J Cell Biol 1999;144:31–43. [PubMed: 9885242]

Wyrick S, McDougald DL, Mailman RB. Multiple tritium labeling of (+)-7-chloro-8-hydroxy-3-methyl-1- phenyl-2,3,4,5-tetrahydro-1H-3-benzazepine (SCH23390). J Label Comp Radiopharm 1986;23:685–692.

Zhang J, Barak LS, Anborgh PH, Laporte SA, Caron MG, Ferguson SS. Cellular trafficking of G protein-coupled receptor/beta-arrestin endocytic complexes. J Biol Chem 1999;274:10999–11006. [PubMed: 10196181]

Non-standard abbreviations

cAMP

cyclic AMP; adenosine 3′ 5′-cyclic monophosphate

A-77636
(1R,3S)-3-(1'adamantyl)-1-aminomethyl-3,4-dihydo-5,6-dihydroxy-1H-2-benzopyran)

DA
Dopamine

DNS
dinapsoline; (8.9-dihydroxy-2,3,7,11b-tetrahydro-1H-naph[1,2,3-*de*] isoquinoline)

GRK
G protein-coupled receptor kinase

HEPES
4-(2-hydroxyethyl)-1-piperazineethanesulfonic acid

RIA
Radioimmunoassay

SCH23390
7-chloro-8-hydroxy-1-phenyl-2,3,4,5-tetrahydro-1H-3-benzazepine

TMx
Transmembrane spanning section X

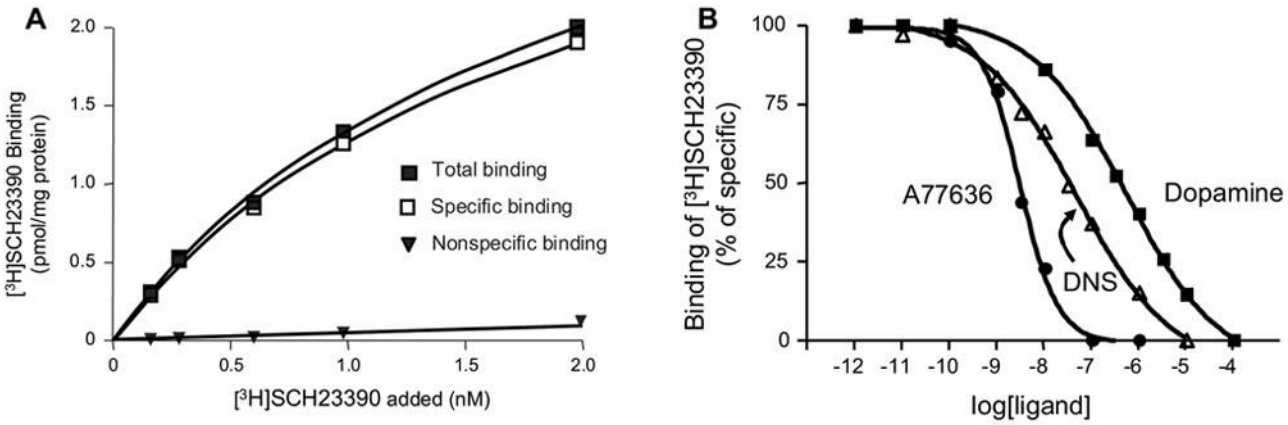

Figure 1. Characteristics of HA-hD$_1$ receptor

(**A**). Saturation binding of [^{3}H] SCH3390 to HA-hD$_1$. Data in Figure were from one of three independent experiments that had a K_D=2.4 ± 0.8 nM; B_{MAX}=4 ± 1 pmol HA-hD1/mg membrane protein.

(**B**). Affinity of dopamine, A-77636, and DNS for the HA-hD$_1$ receptor. Non-specific binding was 17 ± 2.3%. Affinities are summarized in Table I.

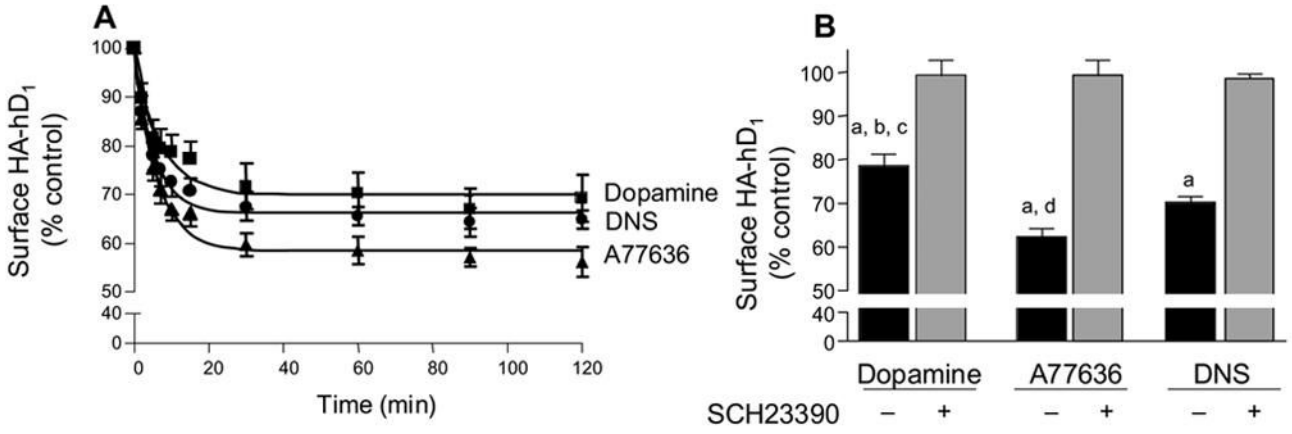

Figure 2. Time course for internalization of dopamine, A-77636, and DNS in HA-hD$_1$ HEK cells

(**A**). HA-hD$_1$ HEK cells were treated with 10 μM dopamine, A-77636, or DNS for 0 to 120 min in quadruplicate. Data are expressed as a percentage of vehicle-treated controls at all time points, and represent the mean and standard errors of three independent experiments. (**B**) Cell surface HA-hD$_1$ remaining at steady state (1 h). HA-hD$_1$ HEK cells were treated with 10 μM dopamine, A-77636, or DNS in quadruplicate for 1 h in the presence of 50 nM -(S)-propranolol and yohimbine. A subset of samples also contained 50 μM SCH23390 in duplicate. Data are expressed as a percentage of vehicle-treated controls at all time points and are the means and standard errors of three to eight independent experiments. A two sample t-test was used to compare samples treated with agonist in the presence and absence of SCH23390 (**a**: $p \leq 0.005$). ANOVA followed by a *post hoc* Tukey test was used to determine significant differences in loss of cell surface receptors after 1 h of treatment with dopamine, A-77636, or DNS (**b**: $p < 0.001$ compared to A-77636; **c**: $p < 0.03$ compared to DNS; **d**: $p = 0.05$ compared to DNS).

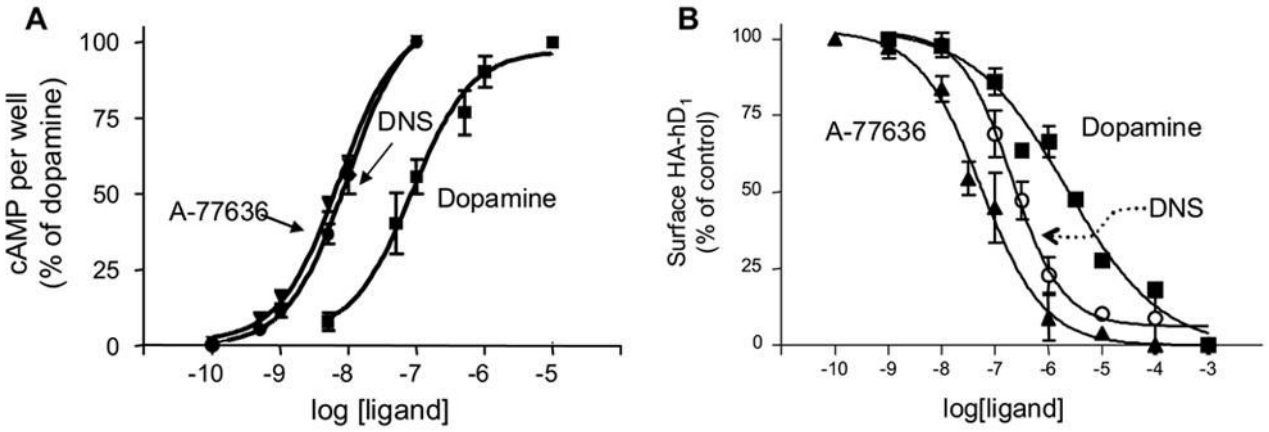

Figure 3. Functional effects of the D_1 agonists

(**A**). Adenylate cyclase functional potency in whole cells. HA-hD_1 HEK cells were incubated with increasing concentrations of dopamine, A-77636, and DNS in quadruplicate. Data are the means and standard errors of four to five independent experiments: EC50 dopamine=91± 47 nM; EC50 A-77636=5.7± 1.8 nM; EC50 DNS=10 ± 3.0 nM. SCH23390 completely blocked activation caused by all three agonists (data not shown).

(**B**). Functional potency of internalization. HA-hD_1 HEK cells were treated with increasing concentrations of dopamine, A-77636, or DNS for 1 h in the presence of 50 nM -(S)-propranolol and yohimbine in quadruplicate. Data are expressed as a percentage of vehicle-treated controls at all time points and were fitted to sigmoidal dose-response curves and EC50s determined by using Prism software: Dopamine=600± 200 nM; A-77636=80 ± 10 nM; DNS=200 ± 100 nM. Data are the means and standard errors of three to six independent experiments.

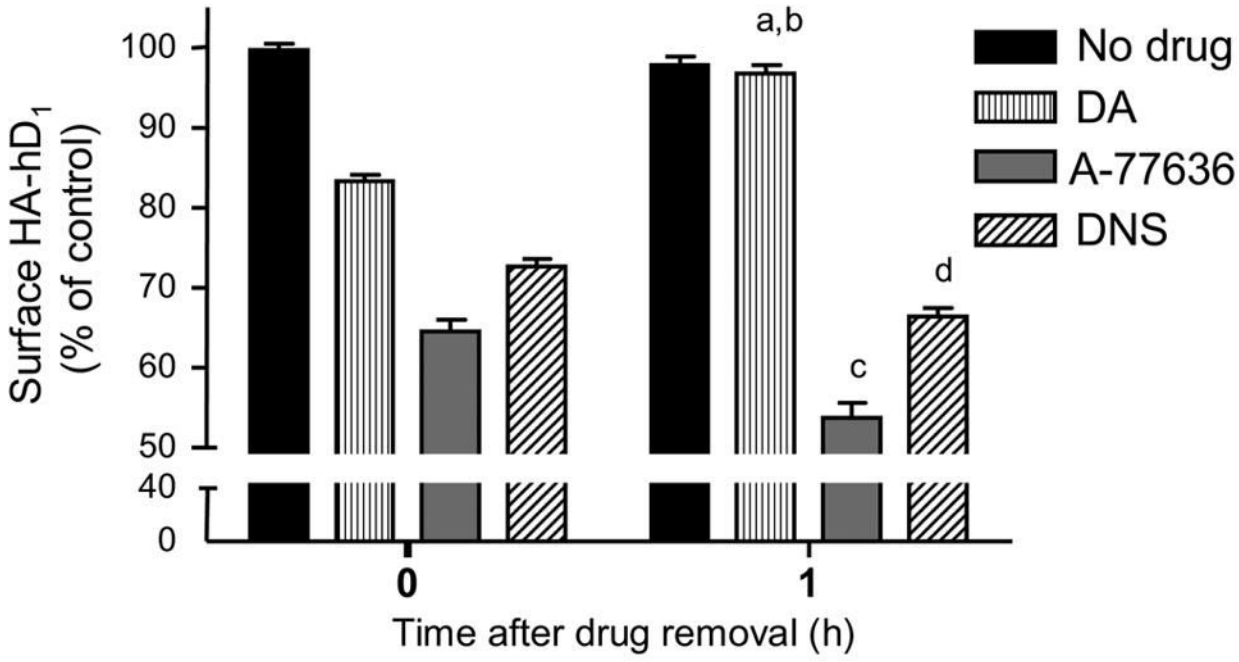

Figure 4.

Recovery of cell surface HA-hD1 1 h after agonist removal. HA-hD1 HEK cells were treated with 10 μM dopamine, A77636, or DNS for 1 h in quadruplicate. A cell surface RIA for the HA tag was used to measure cell surface HA-hD_1 1 h after agonist removal Data are expressed as a percentage of vehicle-treated controls and are the means and standard errors of four to five independent experiments. A one way ANOVA with a post-hoc Tukey test was used to compare dopamine-treated cells at 0 and 1 h after dopamine removal (a, $p<0.001$) and to compare dopamine-treated versus untreated controls at 1 h after agonist removal (b, $p>0.05$). A-77636 and DNS were also compared at 0 and 1 h after removal of these agonists (A-77636: c, $p<0.001$; DNS: d, $p<0.05$).

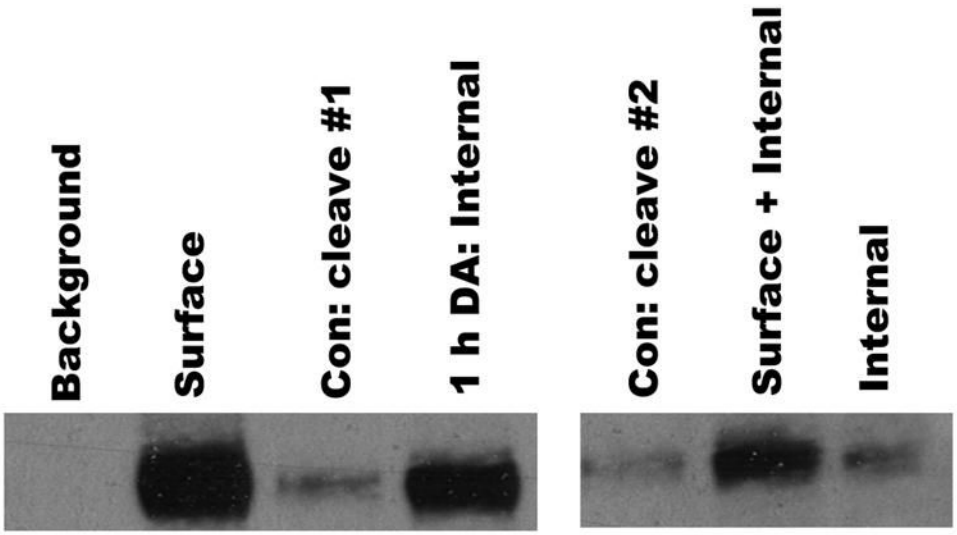

Figure 5.

Reversible biotinylation of cell surface HA-hD$_1$. HA-hD$_1$ HEK cells were biotinylated with a cell impermeable, cleavable reagent. Biotinylated receptor was then tracked in response to DA treatment and removal in duplicate as described in Experimental Procedures. Lane labels are as follows: Background: background binding of non-biotinylated HA-hD$_1$ to avidin resin; Surface: total biotinylation of cell surface HA-hD$_1$ in the absence of DA; Con: Cleave #1: remaining cell surface HA-hD$_1$ after GSH cleavage in the absence of DA (a control for completeness of GSH cleavage); 1 h DA:Internal: internalized HA-hD$_1$ after 1 h of DA treatment and cleavage of cell surface HA-hD$_1$ with GSH; Con: cleave #2: remaining cell surface HA-hD$_1$ after second GSH cleavage (control for completeness of second GSH cleavage); Surface + Internal: total HA-hD$_1$ (internalized and surface) after 1 h of DA treatment followed by 1 h of DA removal; Internal: internalized HA-hD$_1$ remaining after removal of cell surface HA-hD$_1$ by second GSH cleavage (i.e. HA-hD$_1$ that was not recycled).

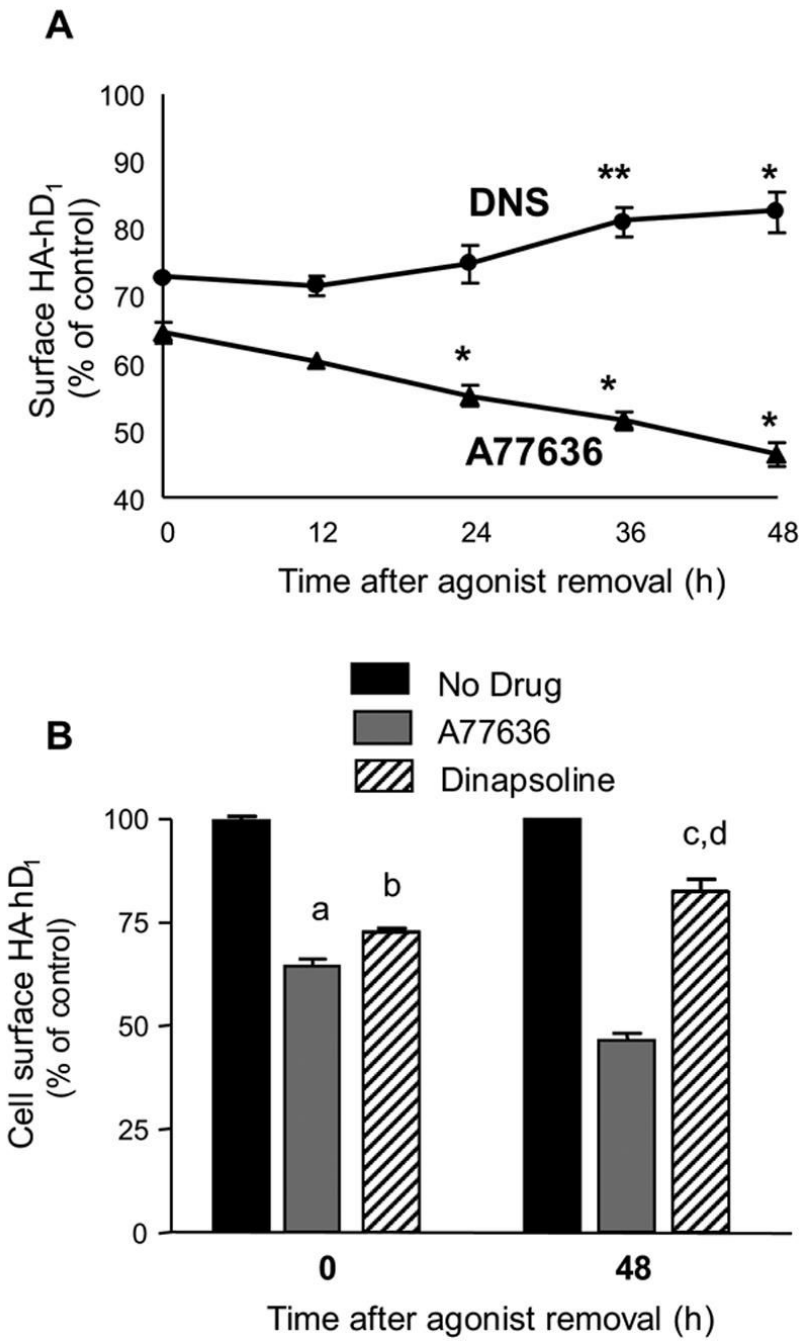

Figure 6. Time effects of changes in cell surface receptors

(**A**). Time course of changes in cell surface HA-hD_1 after removal of A77363 and DNS. Cell surface RIA of HA-hD1 HEK cells treated with 10 μM A-77636 or DNS in quadruplicate for 1 h, rinsed with PBS and incubated in drug-free medium for 0–48 h. Data are expressed as the percentage of vehicle-treated controls at all time points and are the means and standard errors of four to five independent experiments. (*) $p \leq 0.03$, (**) $p=0.08$ compared to t=0.

(**B**) An ANOVA with a post-hoc Tukey test was used to compare A-77636-treated cells at 0 and 48 h after A-77636 removal (a, $p<0.001$) and to compare cells treated with DNS at 0 and 48 h after DNS removal (b, $p<0.05$). At 48 h, DNS-treated receptors are significantly decreased

relative to untreated controls (c, $p<0.001$), but are significantly elevated compared to those treated with A-77636 (d, $p<0.001$).

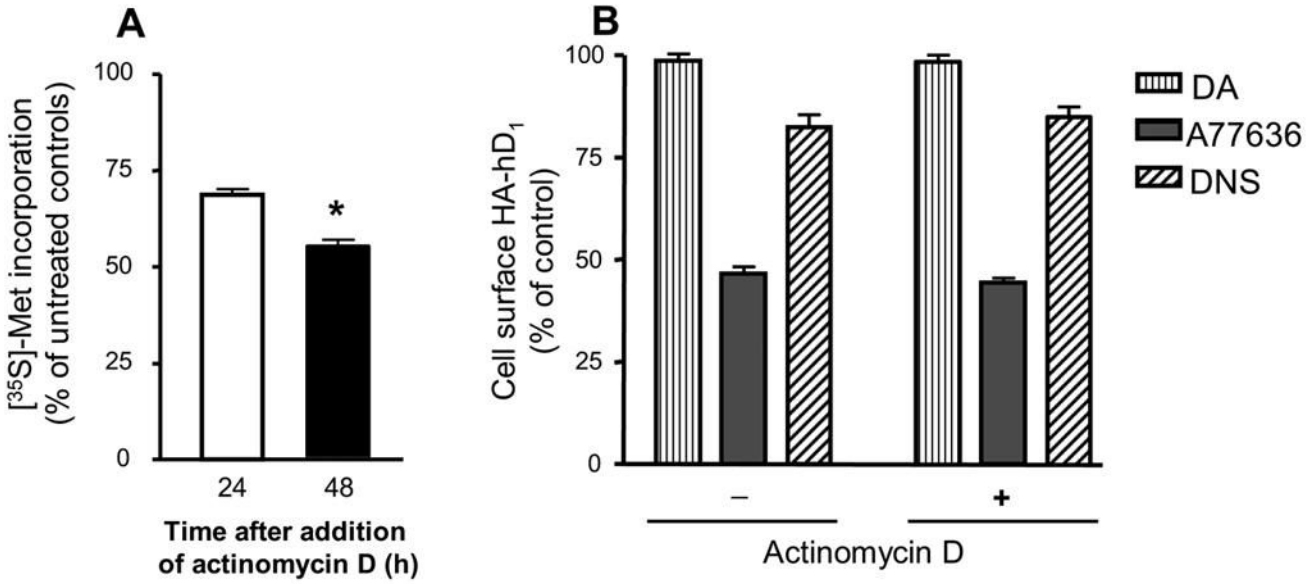

Figure 7. Inhibition of protein synthesis by actinomycin D

(**A**). HA-hD_1 HEK cells were labeled with [^{35}S]-methionine in the presence or absence of 5 μM actinomycin D for 24 or 48 h in triplicate. Similar, unlabeled samples (without the radiolabel) were run in parallel for quantification of viable cells by a spectrophotometric MTT assay. Data were normalized to the absorbance of reduced MTT and are expressed as the percentage of incorporation of [^{35}S]-methionine in untreated controls. A two-tailed t-test was used to compare the extent of label incorporation at 24 and 48 h (*) p=0.008.

(**B**) Actinomycin D does not alter the response of HA-hD_1 to agonist treatment. Cell surface RIA of HA-hD_1 HEK cells treated with 10 μM dopamine, A-77636, or DNS for 1 h in quadruplicate, rinsed, and incubated in drug-free medium in the presence or absence of 5 μM actinomycin D for 48 h. Data were expressed as a percentage of vehicle-treated controls. A one-way ANOVA with a post-hoc Tukey test was used to compare the effects of actinomycin D treatment on receptor density for each agonist at 48 h after agonist removal (p>0.05).

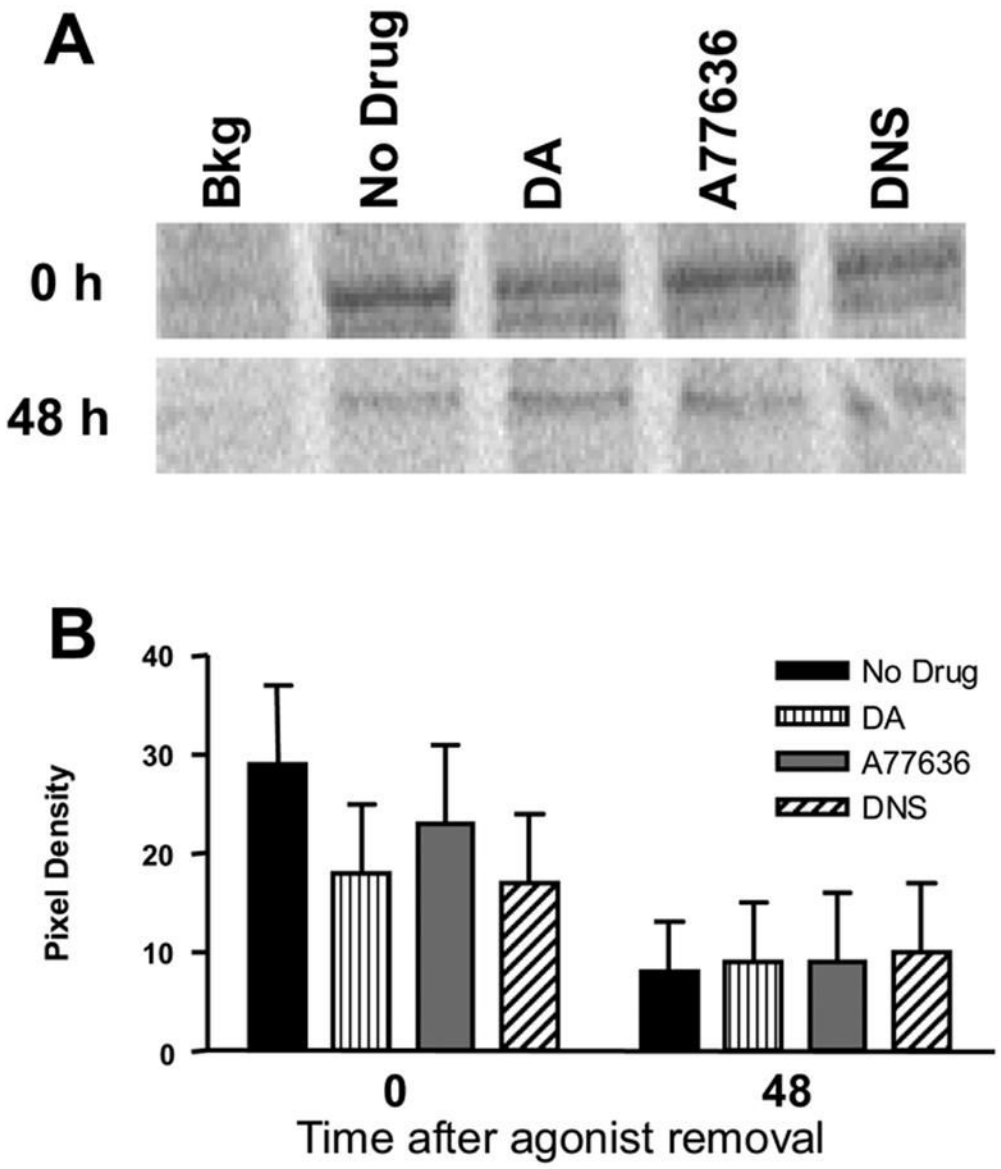

Figure 8. Pulse-chase labeling of HA-hD$_1$ with [^{35}S]-methionine

(**A**). HA-hD1 HEK cells were labeled with [^{35}S]-methionine prior to treatment with agonist or vehicle in duplicate for 1 h and incubation in agonist-free medium for 0 or 48 h. Data are representative of three independent experiments.

(**B**). Graph of the pixel density in each band (above) with standard deviation (corrected for background).

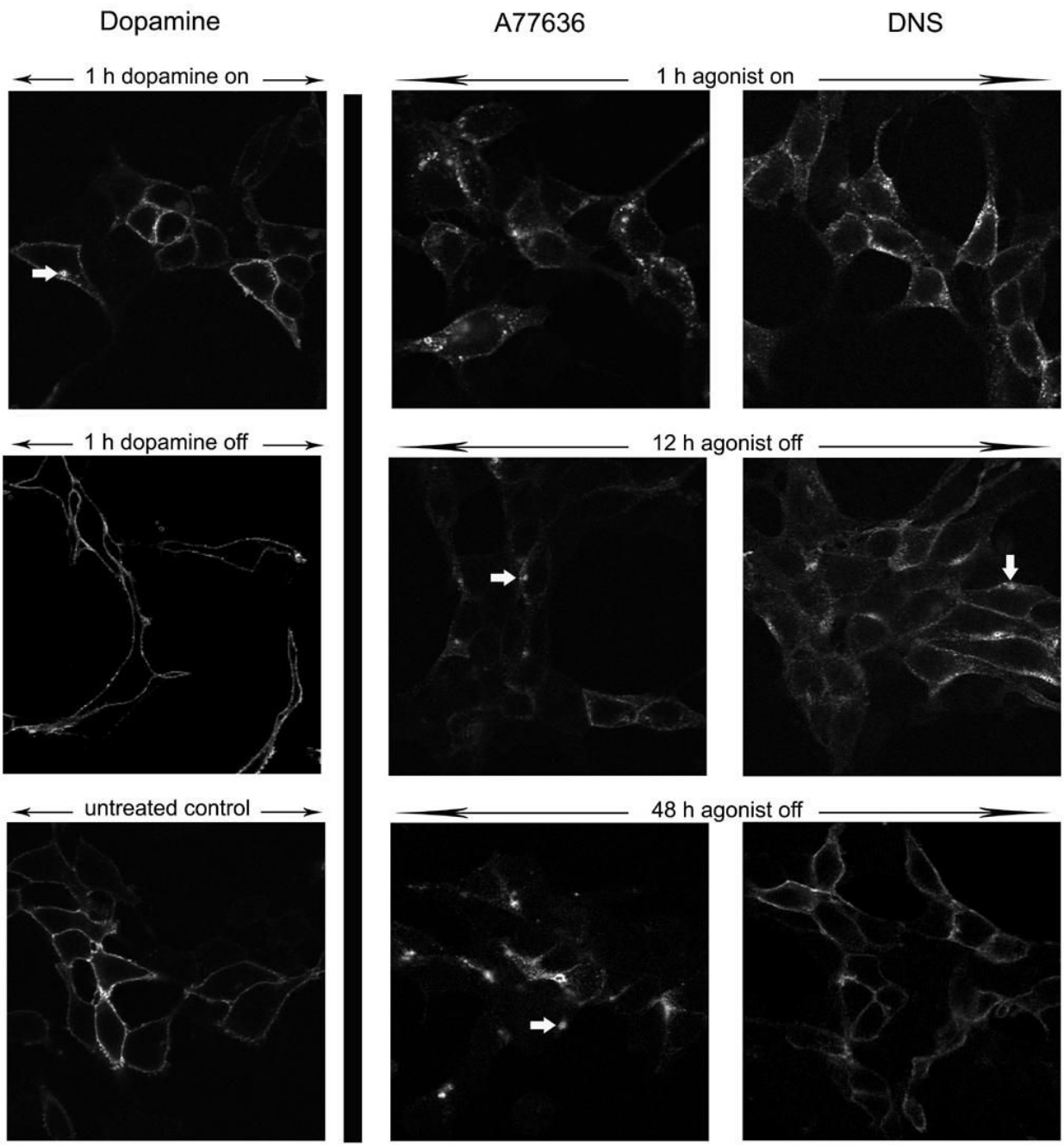

Figure 9.

Visualization of HA-hD$_1$ subcellular localization in response to agonist treatment and removal by confocal microscopy. HA-hD$_1$ staining [HA.11 primary antibody, cy3 secondary antibody converted to grayscale) is localized primarily to the cell membrane in HA-hD$_1$ HEK cells untreated with agonist (top row at left),. The HA-hD$_1$ receptor is localized intracellularly 1 h after treatment with 10 μM agonist (middle row). After washing and incubation in drug-free medium, HA-hD$_1$ staining recovers to the cell surface 1 h after removal of dopamine (middle row at left) and is evident at 48 h after removal of DNS (bottom row at right). No recovery of cell surface HA-hD$_1$ staining is observed in response to A-77636 (second and third row at middle). DAPI staining for cell nuclei was removed to clearly show the receptor. Arrows

indicate a large endosomal-like structure containing internalized HA-hD_1. Data are representative of three independent experiments performed in duplicate.

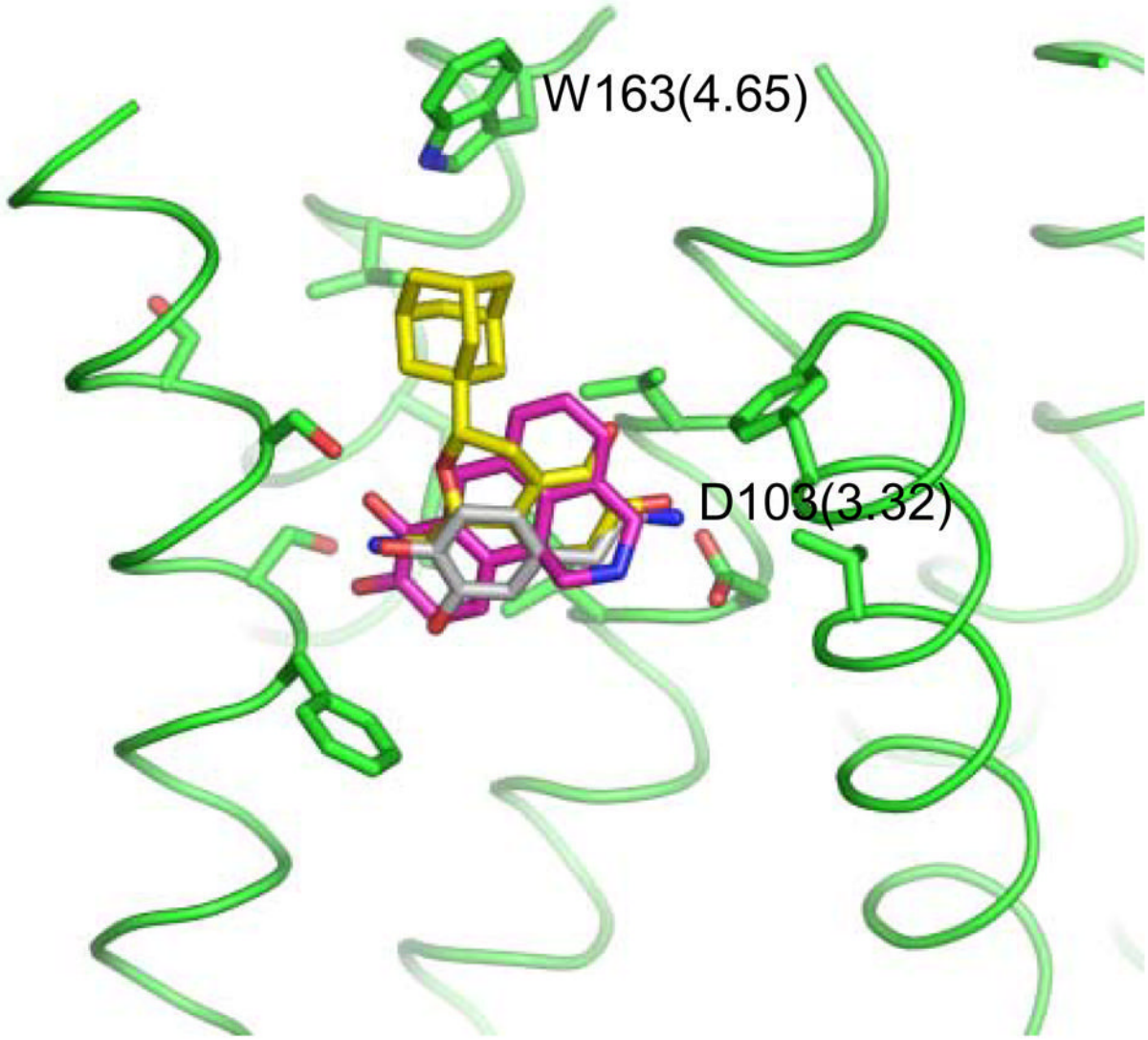

Figure 10.
Predicted docking of dopamine, dinapsoline, and A-77636 to the D_1 receptor located between TM helices 3, 4, 5 and 6. The residues from the extracellular end of the TM regions are predicted to be involved in binding of the synthetic ligands, but not dopamine. Extracellular domain is at the top.

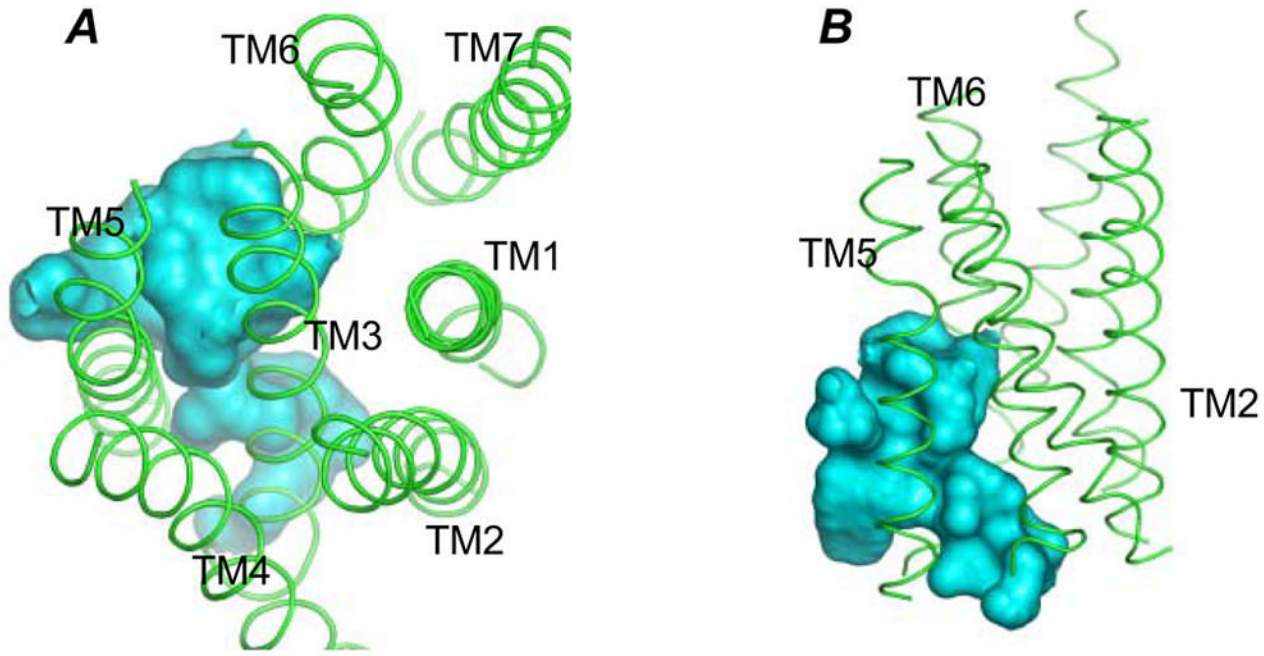

Figure 11.

Panel ***A.*** Top view (from the extracellular end) of the location of the secondary binding site for dinapsoline and A-77636 in human dopamine D_1 receptor. The secondary binding site is postulated as allosteric, and is located at the intracellular half of the TM barrel between helices 3, 4, 5 and 6. Panel ***B***. Side view of the location of the binding site.

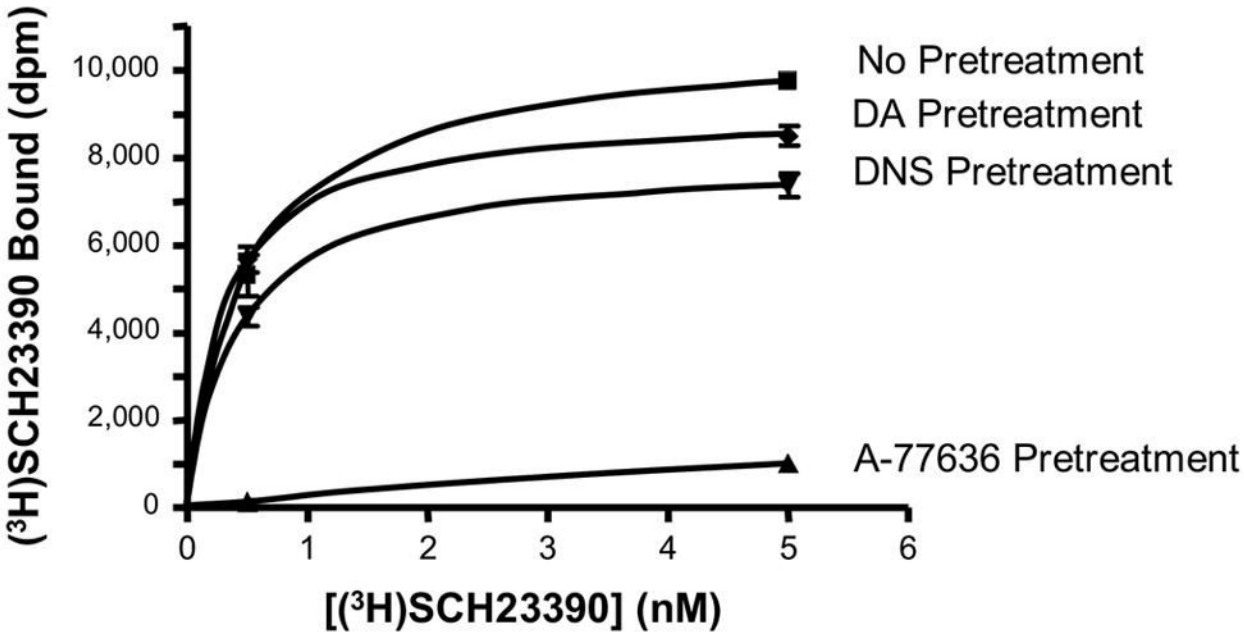

Figure 12.

Inability of [^{3}H]SCH23390 to displace A-77636 in membranes from HEK cells expressing hD_1 receptors. After preincubation with dopamine, dinapsoline, or A-77636, the membranes were washed extensively as described in the Methods. Mini-saturation assays then were performed using [^{3}H]SCH23390 concentrations equal to $1*K_D$ and $10*K_D$. There was almost complete loss of binding caused by the pretreatment with A-77636, but not dinapsoline or dopamine.

Table 1

Summary of ligand binding affinity in HA-hD_1 HEK cells.

Ligand	$K_{0.5}$ (nM)	η_H	K_D(High) (nM)	K_D(Low) (nM)	% High Affinity
SCH 23390	2.4 ± 0.8	1.0	NA	NA	NA
Dopamine	370 ± 1.2	0.34 ± 0.05	17 ± 0.30	2100 ± 38	46 ± 3
A77636	1.77 ± 0.01	1.27 ± 0.13	NA	NA	NA
Dinapsoline	26.8 ± 1.3	0.42 ± 0.07	1.40 ± 0.01	120 ± 4	42± 7

NA = not applicable